Current Chemistry Letters 13 (2024) 49–60

Contents lists available at GrowingScience

Current Chemistry Letters

homepage: www.GrowingScience.com

Insight into a new discovery of SARS-CoV-2 inhibitor activated through Chloroquine derivatives

Mohammed Salah[a], Oumaima El Alaoui El Abdallaoui[b], Abdellah Zeroual[a], Nivedita Acharjee[c] and Mohammed El idrissi[d*]

[a]*Molecular Modeling and Spectroscopy Research Team, Department of Chemistry, Faculty of Sciences, Chouaïb Doukkali University, El Jadida, Morocco*
[b]*Heart Institute, Medical School, University of Pécs, Pécs, Hungary*
[c]*Department of Chemistry, Durgapur Government College, Durgapur, Paschim Bardhaman, West Bengal 713214, India*
[d]*Laboratory of Chemical Processes and Applied Materials, Sultan Moulay Slimane University, Faculty Polydisciplinary Beni-Mellal, Morocco*

C H R O N I C L E

Article history:
Received March 20, 2023
Received in revised form
June 9, 2023
Accepted August 17, 2023
Available online
August 17, 2023

Keywords:
SARS-CoV-2
Chloroquine
Main protease (Mpro)
Papain-like protease (PLpro)
Spike protein

A B S T R A C T

The inhibiting effect of chloroquine compounds (ChCs) on the SARS-CoV-2 virus represents a highly debated form of study owing to the emerging proposals of mechanistic implications for exploring the mode of action of ChCs on the virus. Keeping in view the emerging significance of chloroquine derivatives, the present study was performed to screen one hundred and ninety known chloroquine derivatives for their interaction with several SARS-CoV-2 target proteins by molecular docking and molecular dynamics simulations to obtain an in-depth understanding of the potential hits of these compounds against SARS-CoV-2. A total of 190 molecules from the chloroquine family were screened for the identification of potential new inhibitors of the three therapeutic target proteins of SARS-CoV-2, namely Mpro (master protease), PLpro (papain-like protease) and SGp-RBD (spike glycoprotein receptor binding domain). The ChCs bound to SARS-COV-2 Mpro, PLpro, and SGp-RBD were generated by molecular docking and molecular dynamics simulations. Herein, a comparative analysis of chloroquine family products and a well-known drug against SARS-CoV-2, called Remdesivir, has also been presented. This investigation is intended to study the mechanism of interaction between ChCs and the SARS-CoV-2 virus and explore the unprecedented areas associated with the inhibitory activity of ChCs against this virus.

1. Introduction

The sudden outbreak of highly transmittable and pathogenic viral infections caused by the SARS-CoV-2 virus has imposed a global health emergency with a dramatic loss of human life in the last two years and has undermined the economy considerably. Cytokine and Growth Factor Reviews has published several Special issues since the beginning of the COVID-19 pandemic in 2019-2020, focusing on biology, pathogenesis, and therapeutic options for COVID-19 infection[1]. These issues include articles on the involvement of the chemokine system in the cytokine storm in COVID-19, intervention in the early stages of COVID-19 pneumonia, the therapeutic value of corticosteroid treatment, early clinical intervention with type 1 interferons, progress in vaccine development, and organ-specific complications of COVID-19. By 2022, multiple highly efficacious vaccines are available and being administered worldwide, therapeutic options have been clinically evaluated and approved, and SARS-CoV-2 has become one of the most thoroughly studied viruses in history. However, with progress has also come unanticipated problems[2], such as misinformation, anti-vaxxers, opposition to protective masks, and politically motivated interference disguised as knowledge[3]. The emerging COVID-19 variants underscore the efficacy of the virus in

* Corresponding author.
E-mail address m.elidrissi2018@gmail.com (M. E. Idrissi)

doi: 10.5267/j.ccl.2023.8.010

potentially escaping the immune system, simultaneously enhancing their transmission. Nonetheless, further research is needed to fully understand the impact of these variants on the path of the pandemic.[4]

Herein, several promising agents have been proposed with significant action against the virus, a perfect antiviral product is still awaited to combat the same. Although Chinese researchers have reported the antimalarial drugs chloroquine and hydroxychloroquine to show effectiveness in SARS-CoV-2 patients[4], the conclusive statement on the inhibitory efficacy of chloroquine compounds is yet to receive acceptability from the medicinal community owing to the budding phase of the mechanistic implications that govern the interaction of the target proteins with these molecules.

Elucidating the 3D structure of protein targets of interest in a given disease and then identifying small molecules with the appropriate chemical characteristics to link to the target proteins is an appealing strategy to discover active and effective therapeutic candidates. The main tool for calculating and predicting the binding free energy of a chemical molecule in the pocket of a protein is molecular docking. Traditionally, in silico screening for structure-based drug development has used X-ray crystal structure (docking). This method has recently been used to discover impressive potential modulators of the major SARS-CoV-2 protease using plant compounds[5].

In this paper, we have applied a similar strategy to identify the most promising derivatives of the chloroquine family showing inhibitory effects on SARS-CoV-2, while the study is also intended to comprehend the inhibitory mechanism and pave the way for development of a new generation of molecules with pronounced inhibitory activity and limited adverse effects.

During a global health emergency, the potential use of chloroquine or its analogs as a breakthrough treatment may seem promising. Thus, Chloroquine is a cost-effective and widely regarded as safe drug that has been used for decades. Early in vitro, studies have shown promising results. Currently, Indian Council of Medical Research recommended that hydroxychloroquine is widely used for the treatment of coronavirus infections. CQ and HCQ are the relevant antiviral drugs for the reducing chance of COVID-19 through increased endosomal pH and interference with glycosylation of the angiotensin-converting enzyme 2 (ACE2) receptor[5]. However, there is still a lack of translational investigations to determine its effectiveness in treating COVID-19 in humans. Further research is needed to fully understand the potential benefits and risks of chloroquine derivatives in the context of COVID-19.[3] Thus, chloroquine compounds were first chosen, and high-throughput screening, virtual drug screening, and structure-based drug design were integrated. The main protease (Mpro), the papain-like protease (PLpro), and the SARS-CoV-2 spike protein were examined using ChCs (S-protein). The first protein, Mpro, obstructs viral transcription and replication. The transcription and replication of viruses are facilitated by the second protein, PLpro[6,4]. The coronavirus membrane is protected on the outside by the S-protein, which enables the virus to bind the ACE2 enzyme to host cell membranes, start membrane fusion, and infect the host cell[6].

The goal of the current work is to identify ChCs that are crucial for targeting and interacting with the earlier proteins. A total of 190 ChCs, including licensed medications, drug candidates, and other pharmaceutically active compounds authorized by the World Health Organization (WHO) for clinical trials, were screened from the PubChem database[5]. This work helps to clarify the unclear aspects associated with the inhibitory efficacy of chloroquine derivatives against the virus. It is also worthwhile to look into the possibility of developing new medications to combat the SARS-CoV-2 virus.

2. Materials and methods details

2.1 Data bank of chloroquine family and selecting

For the present study, the selected chloroquine family database consists of 190 compounds from the PubChem database[5] that may represent a potential molecule against the SARS-CoV-2 virus. Our selection procedure is based on the Canvas package[6] of Schrödinger software (Canvas, Schrodinger, LLC, New York, NY, 2020). The selected criteria for study are molecular weight, hydrogen bond donors, partition coefficient log P, polar surface area, and rotatable bonds. The number of atoms has been considered between 20 and 70, and the molar refractive power is between 40 and 130. The above selection rule swallowed appropriate filtering of the chloroquine family collection.

1.1. Proteins and ligand preparation

The proteins 6LU7 (major protease)[10], 6W41 (spike protein)[11], and 6W9C (papain-like protease: PLpro)[12] were selected as the target proteins, as reported in the literature and characterized by the X-ray method with a resolution higher than 2.5. The X-ray coordinates of the Mpro, Spro, and PLpro proteins were taken from the PDB database (**Fig. 1**)[13].

Protein	Binding site	Ref.
3CLpro	HIS41, MET49, PHE140, GLY143, SER144, CYS145, HIS163, GLU166, PRO168, GLU189	[14]
PLpro	Asp164, Val165, Arg166, Glu167, Met 208, Ala246, Pro247, Pro248, Tyr 264, Gly266, Asn267, Tyr 268, Gln269, Cys217, Gly271, Tyr273, Thr301 and Asp302	[15]
S protein	L455, F486, Q493, S494, N501	[16]

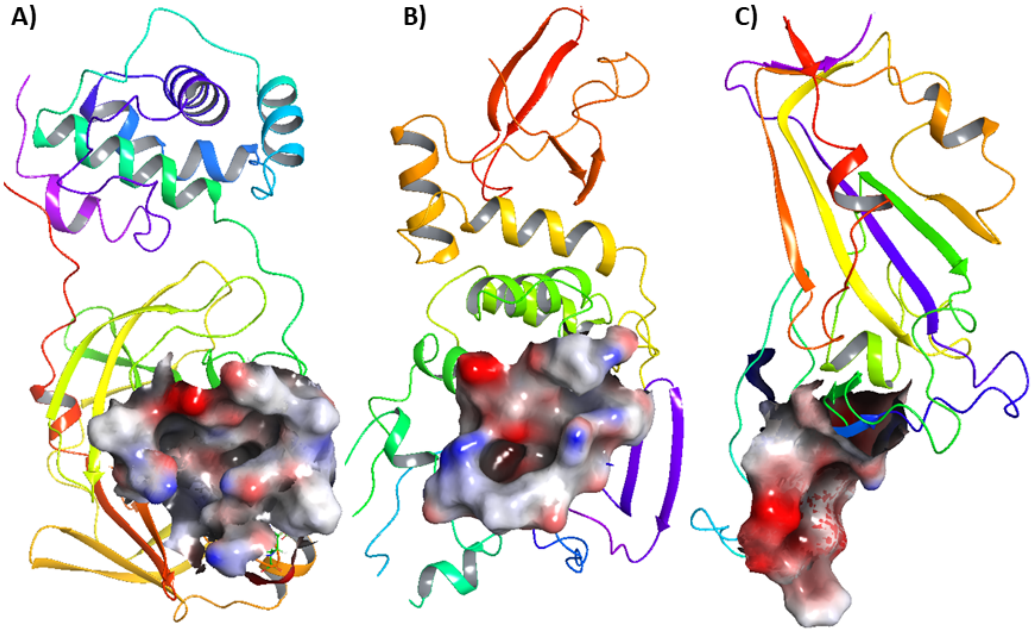

Fig. 1. 3D-structure of the binding site of each protein: **A)** Mpro, **B)** PLproand and **C)** Spro

To refine the structure, we used the Maestro version 18.1 protein preparation wizard, removing the water and optimizing the H-bonding. Minimization of the heavy atom molecule at an RMSD of 0.30 was done using the OPLS3 force field. For this study, the chloroquine derivatives have been used on the basis of a WHO report mentioning chloroquine and its analogue hydroxychloroquine to have excellent activity against[11,12] SARS-CoV-2 and reported as the potential inhibitors to target SARS-COV-2. The investigation was started with 190 ligands, which were docked to further identify them as a probable lead structure for a drug against three exotic proteins in the life cycle of SARS-CoV-2. The preparation of the ligands was done to achieve a stable conformation. The application Ligprep (Schrödinger 2018-1) was used to obtain a stable structure of the ligands in terms of stereochemical properties (Schrödinger Suite: LigPrep, version 2.5; Schrödinger, LLC: New York, 2012) [16]. Polar hydrogen atoms were added to the crystal structures of the protein, followed by the addition of Kollman and Gasteiger charges atoms. Finally, pdbqt files of ligands and protein were generated. The grid box with radius of 60 × 60 × 60 $Å^3$ in x, y and z directions was generated and the dimensions of the active site coordinates are -10.729 Å, 12.418 Å and 68.816 Å by the ligand location in the protein.

2.2 Binding site

Maestro version 18.1 glide generation was used to create the receptor grid for protein-ligand interaction, while OPLS3 was used as the force field. A scaling factor of 1.00 was set for the Van der Waals radius scale and a cutoff of 0.3 for the charge. The centroid of the active site residues was used to generate a cubic box of appropriate size for the receptor. A precise limiting box was established for each protein to assess docking processes. The amino acids injected for the grid generation method were implemented for each protein to prepare the binding site, which is the center of all these amino acids, and are shown below.

2.3 Docking screening

Starting with the entries 6Y2E (main protease)[17], 6W41 (spike protein)[18] and 6YVA (papain-like protease)[16] in Protein Database Bank, the Schrödinger software was implemented to prepare each target. The Protein Structure Preparation Wizard of the Schrodinger programm[16] was used to first process the crystal structure before a docking grid was made. With the exception of rewarding intramolecular hydrogen bond formation and enabling conjugated π-group planarity enhancement, flexible glide docking was carried out using the default settings. On CYS145, the co-crystalline ligand N3 was covalently attached. We then investigated whether the flexible docking of Glide could reproduce the native binding position. Chloroquine, a potent inhibitor of malaria protease[15], has been shown to be effective in treating SARS-CoV-2 patients. Therefore, the present theoretical investigation is focused on the chloroquine family. Thus, we prepared 190 chloroquine derivatives from the PubChem database[20]. The docking boxes were created using the grid generation implemented in the Schrodinger software.

The complete receptor binding domain (RBD) of ACE2 was built into a sizable box and related to PDB ID: 6VW1 in the case of the spike protein. Smaller boxes were placed around the catalytic sites of the two proteases, and a bigger section included the S1 and S2 sites in the main protease's binding pocket. The following HVS filter, MM-PBSA, received the best hits from the docking screens[21]. The Maestro software's protein preparation wizard was used for the same approach to prepare the other two proteins (Mpro and PLpro).

2.4 MM-PBSA-WSAS Binding Free Energy

For the estimation of the binding free energy, each pose of the top-picked compounds was chosen equally. Without doing any additional minimization, the molecular mechanical (MM) energy (EMM) and MM-PBSA free energy of solvation were calculated for each chosen pose[22,23]. The following are the fundamental criteria used to validate the MM-PBSA-WSAS analysis: The surface tension used to get the nonpolar solvation energy is 0.054, the internal dielectric constant is 3.9, and the external dielectric constant is 80. We used the Delphi software (http://compbio.clemson.edu/delphi) to do the MM-PBSA solvation calculation with parse radii[24]. A technique termed WSAS (weighted solvent accessible surface area), published by Wang et al.[25], was used to compute the entropic term. The entropic contribution to this protein target should be acknowledged.

2.5 Molecular dynamics

Based on the outcomes of the molecular docking, the crystalline structures of Mpro, Spro, and PLpro were chosen from the Protein Data Bank (www.rcsb.org) and the two selected organic compounds, and the dynamic response of these structures was examined using molecular dynamics simulations (MD). The comparative molecular dynamics simulation was carried out in three pairs of experiments where (I) compound 01/02-3Mpro, (II) compound 01/02-Spro, and (III) compound 01/02-PLpro were explored separately and their results were compared in order to validate the molecular docking results. After the steepest drop, energy minimization was carried out for both systems. Before beginning the MD run, the systems were equilibrated for 50 ns at 300 K under NVT conditions (constant particle number, volume, and temperature). After the NVT test was finished, the system underwent a 50 ns NPT simulation run with a constant quantity of particles, pressure, and temperature. The trajectories were examined in terms of gyration radius, root mean square deviation, and root mean square fluctuation (Rg, RMSD and RMSF). The GROMACS 'gmxrms', 'gmxrmsf', 'gmx gyrate', and 'gmxhbond' programs were used to count the number of H-bonds created between the ligand and the proteins. The kinetics of hydrogen bonds between the ligand and the protein determine the stability of the ligand-protein system. The dynamics of the hydrogen bonds between the ligand and protein as a function of time characterize ligand-protein stability. The diagrams were produced using the XMgrace tool[26].

3. Results and discussion

3.1 Docking calculations

The binding free energy XP score and log P values of the reference compound Remdesivir and the four chloroquine compounds are shown in Table 1. The estimated binding affinity of Remdesivir (-7.45 kcal/mol) is higher than that of compounds ID 175494, ID 592566, and chloroquine, except that of the derivative compound reported at ID 456355, showing excellent affinity relative to Remdesivir for binding to all our targets, especially to the major protease (-8.07 kcal/mol). By assessing a compound's molecular lipophilicity or hydrophilicity, the log P parameter helps scientists understand how substances cross cell membranes. According to Lipinski's rule[27], a high log P value indicates poor absorption and low permeability, while a low log P value is associated with high absorption and permeability. For a good drug, the log P value should be between -2 and 5. The log P values of our preparations are lower than 5 and higher than -2, revealing that our preparations show good permeability and absorption (Table 1).

Table 1. The XP score free energy of binding and the logP values of the four Chloroquine compounds and Remdesivir

PubChem ID *		Mpro	PLpro	Spro	LogP
456355	**A**	**-8.07**	**-5.872**	**-5.810**	**1.277**
175494	**B**	-7.109	-4.909	-6.102	-0.623
592566	**C**	-7.321	-3.999	-4.963	1.444
Chloroquine		-5.165	-7.297	-3.260	4.346
Remdesivir		**-7.450**	**-6.817**	**-4.808**	**2.364**

As shown in Table 1, compound ID456355 shows significant activity (-8.07 Kcal/mol) against the main protease, better than Remdesivir (-7.450 Kcal/mol) and also against the other two targets, while the other two compounds show activities of -7.109 and -7.321 Kcal/mol, respectively, which are higher than that associated with the binding of chloroquine molecule to Mpro (-5.165 Kcal/mol). After evaluating the binding affinities and partition coefficient (Log P) of our compounds with all three targets, the complementarity between the surface of the compounds and the binding site was subsequently studied, which allowed visualizing the 3D interaction of our compounds in the binding pocket of the three key proteins (**Fig. 2**).

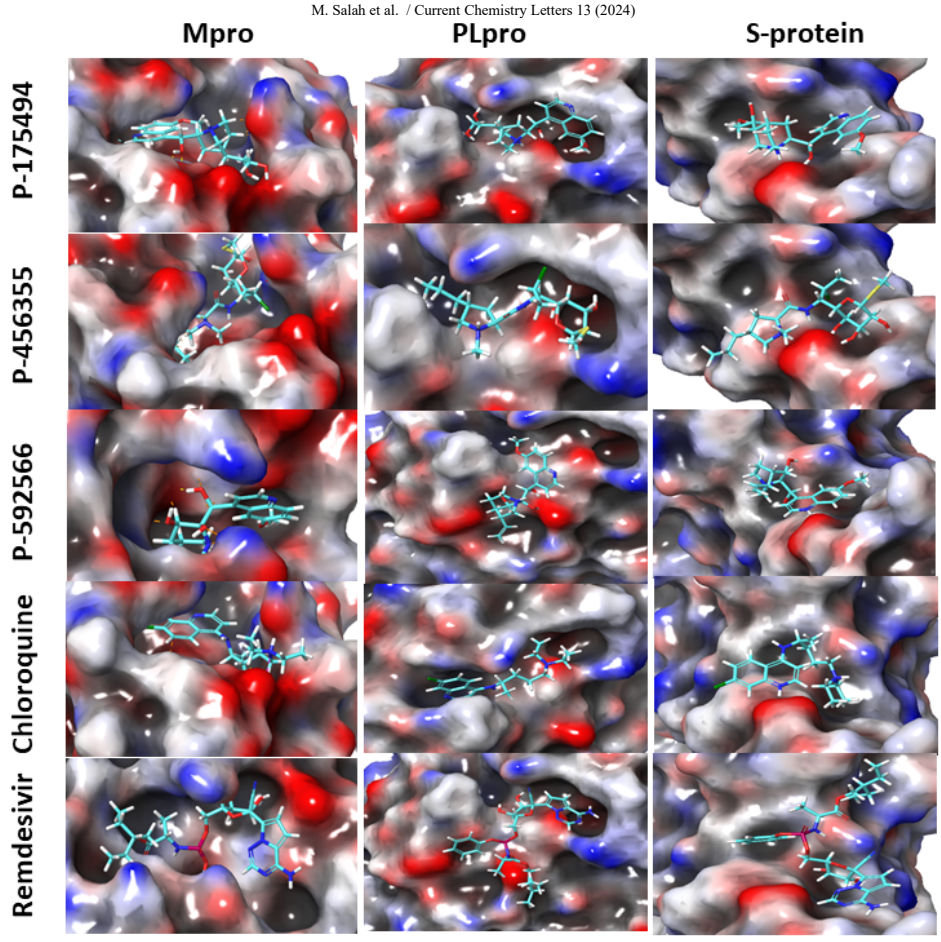

Fig. 2. 3D-Visualization of the studied compounds in the binding site of the three proteins Mpro, Spro and PLpro

The present analysis was further extended to evaluate the binding of amino acids to our compounds and compare the same with the amino acid binding to Remdesivir. Statistical studies indicate that the majority of amino acids interact in the pocket of the protein with a hydrophobic or polar character. The present docking (**Fig. 3**) study and available literature reports reveal two catalytic amino acid residues (HIS41 and CYS145) of great interest for inhibition of the main protease, while the additional residues are GLY143, CYS145, HIS163, HIS164, GLU166, PRO168, and GLN189 reported by Zhang et al[14].

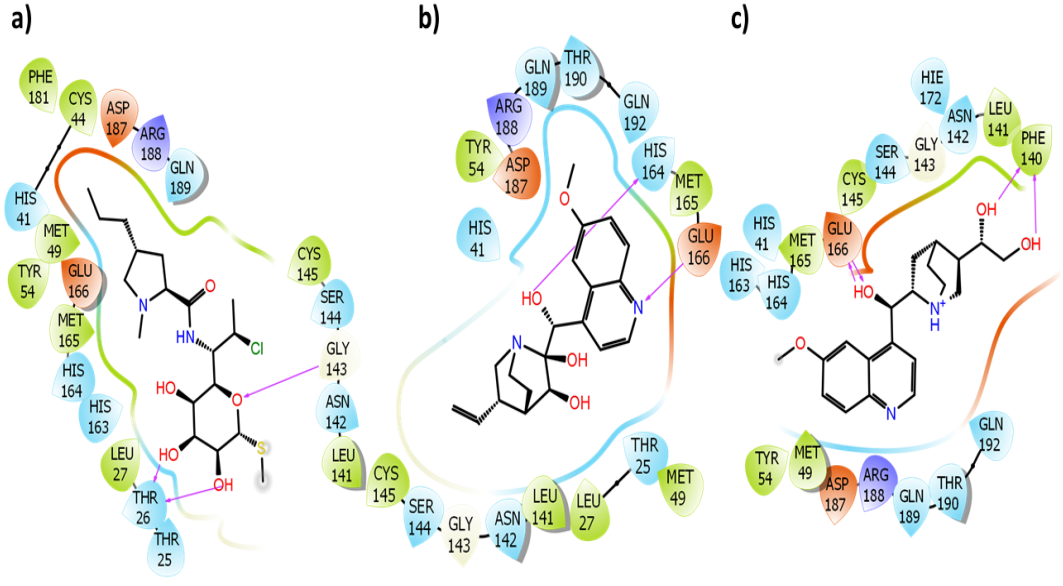

Fig. 3. 2D-structure of the compounds with in the binding site of the Main protease: **a)** P456355, **b)** P17175494 and **c)** P592566

The details of the same for the other two compounds are given in the Binding Site Identification Section. To evaluate the binding of compounds in the active site of each protein, we carefully presented each compound in the binding pocket of three target proteins to study the free energy and activity and visualized the 2D interaction of the compounds in the binding pocket of the proteins. We found that these compounds form more than one hydrogen bond with each of them, as evident from **Fig. 4** and **Fig. 5**.

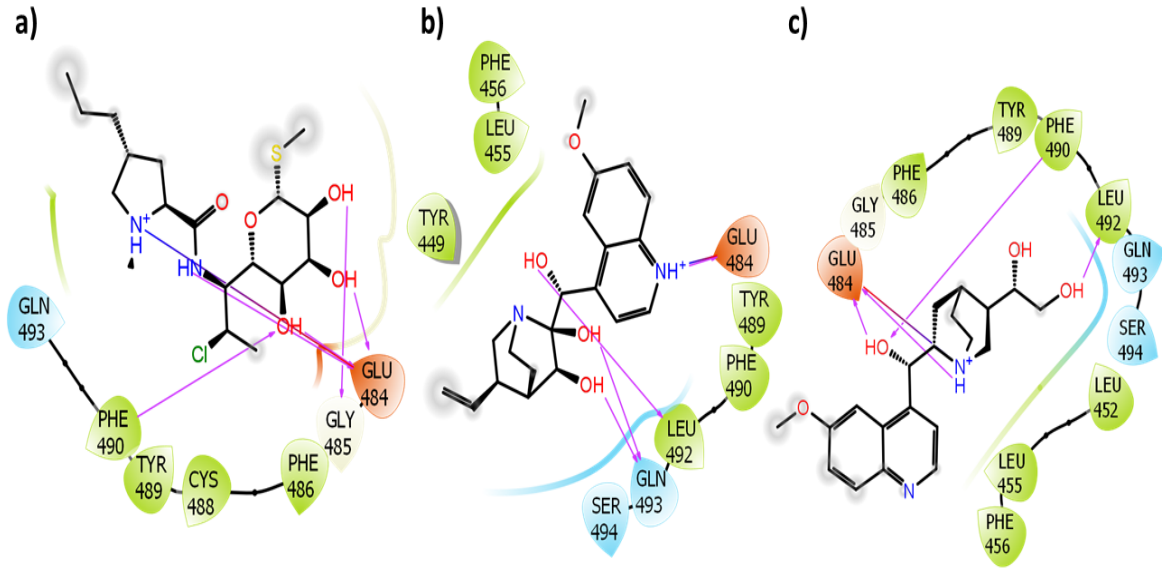

Fig. 4 2D-structure of the compounds within the binding site of the Spike protease:**a)** P456355, **b)** P17175494 and **c)** P592566

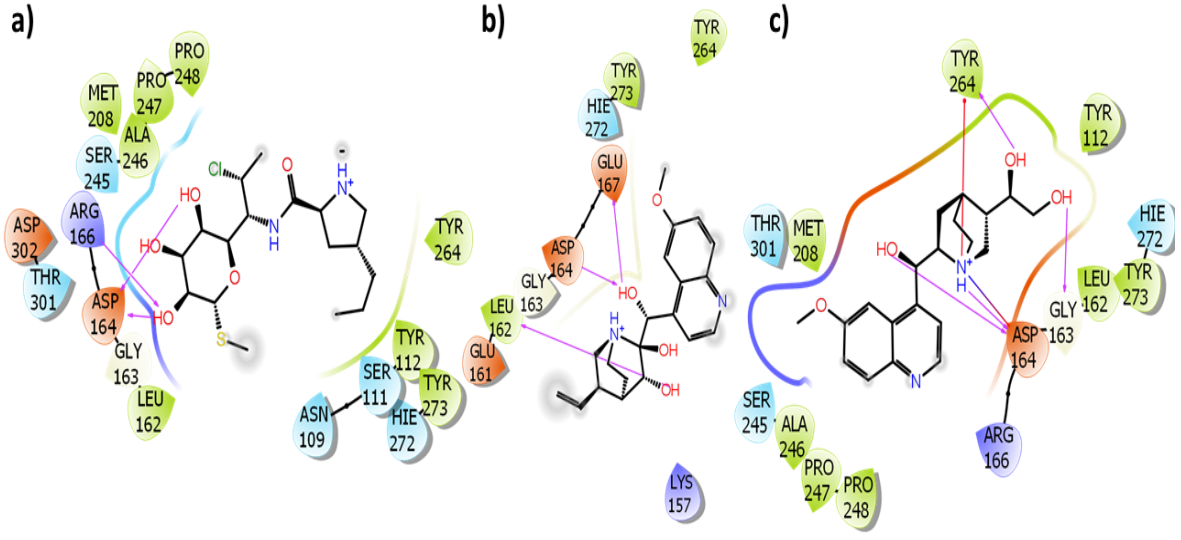

Fig. 5 2D-structure of the compounds within the binding site of the Papain-like protease: **a)** P456355, **b)** P17175494 and **c)** P592566

Fig. 4 shows the most interactive amino acids that have potent significance in the inhibition mechanism of the spike protein of SARS-COV-2(GLU484, GLY485, PHE490, LEU492, and GLN493). The obtained results are in complete agreement with the reported literature[25]. Recent studies show that a region lies in the SARS-COV-2 receptor binding motif (RBM) of the 9 amino acid long sequence 480Cys-Asn-Gly-Val-Glu-Gly-Phe-Asn-Cys-488, which are active residues essential for binding[29]. This region can also be targeted by alternative pathways to inhibit SARS-CoV-2 invasion of the host cells. The SARS-CoV-2 protease plays a dual role, namely the viral replication and inhibition of recognition by the innate immune system. To generate a functional replicase complex, PLpro is required for the processing of the SARS-CoV-2 polyprotein into mature subunits and therefore plays a critical role in the life cycle of SARS-CoV-2[26]. Consequently, its inhibition halts the growth of the disease and is important for combating the pandemic situation. As evident from **Fig. 5**, the compounds bind to LEU162, GLY163, ASP164, ARG166, GLU167, and TYR264 of the PLpro binding site, causing inhibition of this protein. It is noteworthy to mention the study by Rut et al.[30], which reports that the regions remain in the

deepest parts of the pocket of papain-like protease, especially an acidic spot generated by Asp164, Tyr273, and Thr301, which can be used to develop more promising inhibitors.

3.2 Molecular dynamics

Herein, the MD simulation results have been analyzed using different tools to know whether the system is stable, to assess the relevance of protein movements, and to explore the existence and relevance of the interaction. Because drug interaction at the active site of proteins can result in considerable conformational changes, the RMSD (Root Mean Squared Deviation) from the original structure is a regular physical characteristic that enables detection of the structure's conformational fluctuations by MD[31,32]. The protein's molecular structure construction in relation to its initial conformation can be studied using the RMSD[30]. The RMSF provides an understanding of the region of the protein that fluctuates during simulation and was used here to determine the flexibility of all residues to better understand the influence of ligand binding on the flexibility of the protein[31]. The gyration radius (Rg), a measure of the protein's compactness and the stability of its secondary structures when assembled in a compact manner in its three-dimensional (3D) structure, is related to the protein's tertiary structural volume[33]. The stability of the docked complexes is confirmed by the quantity of hydrogen bonds that exist between the complexes and the solvent, which is a good indicator of efficient protein folding. As opposed to the solute, the solvent contains fewer hydrogen bonds while the solute contains more[32]. During 50 ns MD simulations, the hydrogen bonds formed between the complex and water, the solvent environment, within 0.35 nm, were estimated. Interestingly, these molecular dynamics findings, which are displayed in Figures 6, 7 and 8, support the stability of the complexes created by two hits, particularly compound-a (C01) and compound-b (C02) (ID-456355 and ID-175495), with the target proteins Mpro, PLpro, and Spro.

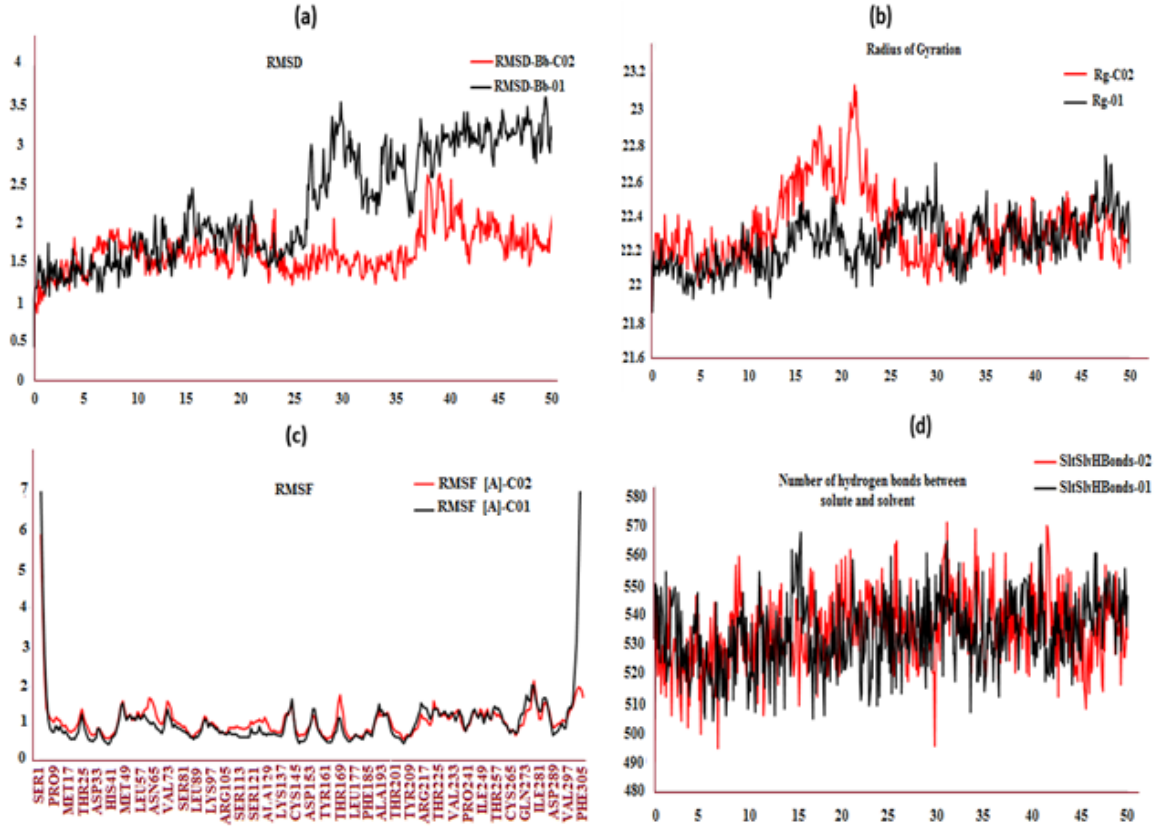

Fig. 6. Representation of **(a)** Mpro backbone RMSD during interaction with C01 (black) and C02 (red), **(b)** Radius of gyration of Cα atoms of Mpro of SARS-COV-2 in the presence of C01 (black) and C02 (red), **(c)** RMSF values of Mpro backbone during its interaction with C01(black) and C02 (red), and **(d)** Number of hydrogen bonds formed by C01 (black) and C02(red) with Mpro of SARS-COV-2 during simulation

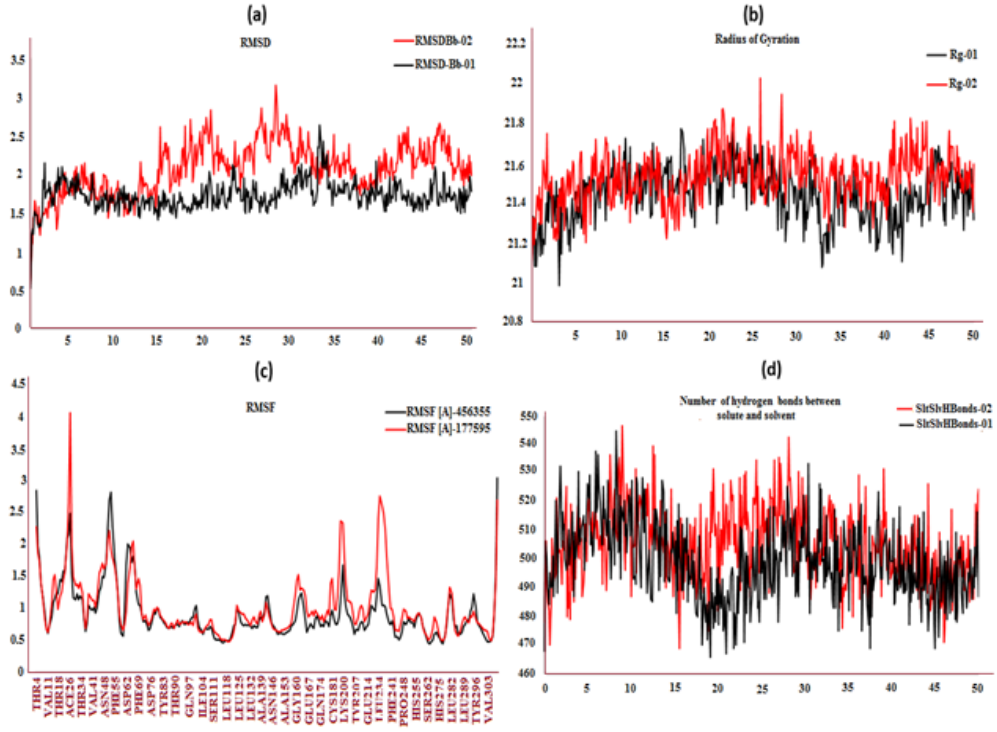

Fig. 7. Representation of **(a)** PLpro backbone RMSD during interaction with C01 (black) and C02 (red), **(b)** Radius of gyration of Cα atoms of PLpro of SARS-COV-2 in the presence of C01 (black) and C02 (red), **(c)** RMSF values of PLpro backbone during its interaction with C01(black) and C02 (red), and **(d)** Number of hydrogen bonds formed by C01(black) and C02(red) with PLpro of SARS-COV-2 during simulation.

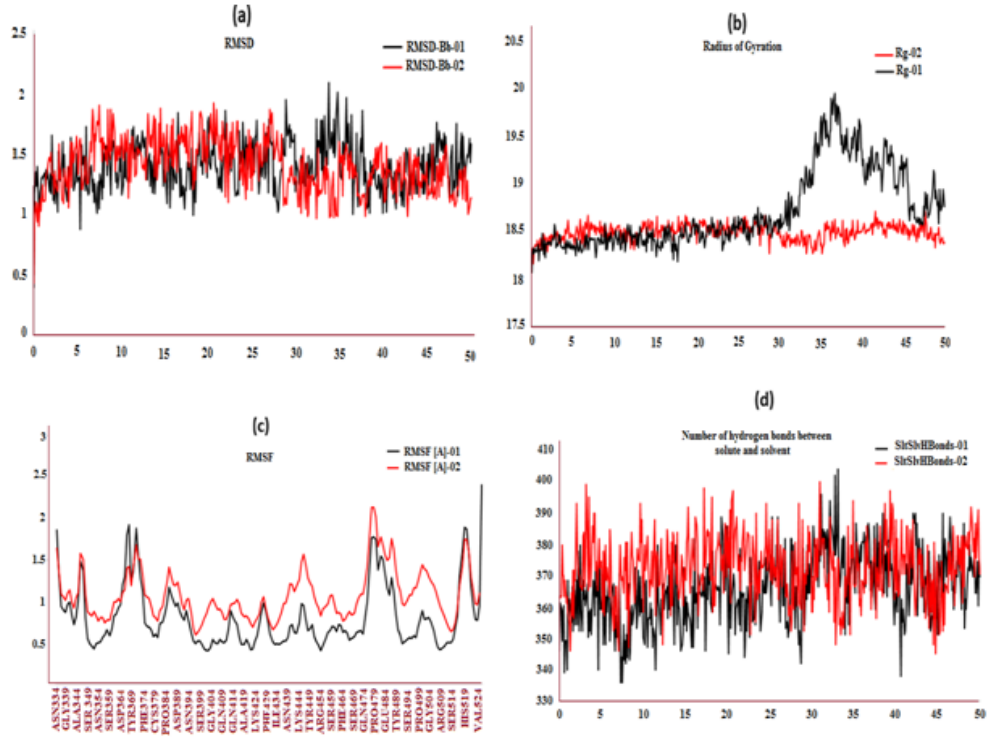

Fig. 8. Representation of **(a)** Spro backbone RMSD during interaction with C01 (black) and C02 (red), **(b)** Radius of gyration of Cα atoms of Spro of COVID-19 in the presence of C01 (black) and C02 (red), **(c)** RMSF values of Spro backbone during its interaction with C01(black) and C02 (red), and **(d)** Number of hydrogen bonds formed by C01(black) and C02(red) with Spro of COVID-19 during simulation

3.3 Mpro molecular dynamic test

The RMSD values of protein backbones in the presence of both ligands reveal higher stability of Mpro in the presence of C02 relative to C01, while the RMSD values get nearly comparable as the system stabilizes after 50 ns of MD run (**Fig. 6 (a)**). In order to understand the degree of compaction in the Mpro structure in the presence of C01 and C02, the radius of gyration (Rg), defined as the mass-weighted root mean square distance of a group of atoms from their common center of mass, was found. **Fig. 6** depicts the calculated Rg values for (i) C01-Mpro and (ii) C02-Mpro along the simulated time scale (b). The Rg value of C01-Mpro and C02-Mpro ranges between 22 and 23 in the first 25 ns before stabilizing at 22.2 in the last 25 ns. The Rg figure indicates that C01-Mpro has slightly lower Rg values than C02, but the difference is not very large. This suggests that the protein operates equally when C01 and C02 are present. The mean, indicating variation in flexibility among residues, is revealed by the RMSF for the typical MD simulation confirmation. The flexibility of the backbone structure in the presence of both ligands was explained by computing the RMSF of the backbone atoms of each amino acid in C01-Mpro and C02-Mpro, which also illustrates how the protein works in the presence of dual ligands. In the presence of both ligands, C01 and C02, the RMSF of the protein backbone Mpro was nearly equivalent, showing that the proteins have a similar affinity for binding. The protein is free to produce higher RMSF values in the case of poor binding, which is not the case in this instance (**Fig. 6** (c, d)).

The stabilisation of ligand-protein complexes depends critically on the proportion of hydrogen bonds that are generated between the complex and the solute. The number of hydrogen bonds formed between the solvent and the solute throughout the simulation at 300 K for the ligated system was used to determine the stability of the hydrogen-bonded arrangement created by C01-Mpro and C02-Mpro. The results are displayed in **Fig. 6.** (d). The hydrogen bond count for the C01-Mpro and C02-Mpro complexes averaged 530 over 50 ns, and it remained constant until the completion of the MD run. The whole scenario predicts that both ligands create sufficient hydrogen bonds and fit into the binding cleft.

Comparing the above results with the recent studies[4], it confirmed that the complex could keep stable throughout the simulation and interact well with the SARS-CoV-2 main protease (MPro), since the RMSD of the ligands indicates a good stability of the system with an average between 1Å and 1.5 Å which is more stable than those demonstrated by the literature[34], Also, the RMSF indicates that the binding of ligand to protein showed well stable interaction and did not result in a large movement in protein conformation as it varies between 1 Å and 2 Å as well as the Rg indicating steady conformation changes of the protein with an average less than 22.2 Å which revealed a more stable results results than those founded by *Rahimasoom Reza[34].*

3.4 PLpro molecular dynamic test

The RMSD values of protein backbones in the presence of both ligands reveal higher stability of PLpro in the presence of C01 relative to C02, while the RMSD values get nearly comparable as the system stabilises after 50 ns of MD run (Fig. 7 (a)). Figure 7 depicts the calculated Rg values for (iii) C01-PLpro and (vi) C02-PLpro along the simulated time scale (b). The Rg values of C01-PLpro and C02-PLpro range from 21.1 nm to 22 nm. The Rg plot indicates somewhat lower Rg values in the case of C01-PLpro; nevertheless, the difference is not statistically significant, implying similar behaviour of the protein in the presence of C01 and C02. The RMSF for the average MD simulation confirmation reveals a mean representing variance in flexibility among the residues.

The flexibility of the backbone structure in the presence of both ligands was explained by computing the RMSF of the backbone atoms of each residue in the (iii) C01-PLpro and (vi) C02-PLpro. The protein backbone PLpro's< RMSF was approximately similar in the presence of both ligands, C01 and C02. The protein is free to produce higher RMSF values if the binding is weak, which is not the case in this instance (**Fig. 7(c, d)**). The stabilisation of ligand-protein complexes is controlled by the number of hydrogen bonds that are generated between the complex and the solute. Based on the quantity of hydrogen bonds between solvent and solute, the stability of the hydrogen bond arrangement created between I C01-PLpro and (ii) C02-PLpro throughout the simulation at 300 K for the ligated system was assessed. The results are displayed in **Fig. 7.** (d). The C01-PLpro and C02-PLpro complexes show between 470 and 540 H-bonds within the first 30 ns, and then only 480 H-bonds at the end of the MD run, demonstrating the strength of the hydrogen bonds between the ligands, particularly C01 and PLpro.

Other in silico studies[4] have also identified chloroquine derivatives as potential COVID-19 PLpro inhibitors, demonstrating minimal deviation and fluctuation based on their RMSD and RMSF values. These values range between 1 Å and 3 Å, and between 0.5 Å and 4 Å, respectively. This consistency aligns with literature[35]. Additionally, a higher Rg value of a protein molecule indicates loose packing within its structure, while a lower Rg value indicates tight packing. The Rg values observed in **Fig. 7** are all less than 22 Å, which is favorable when compared to those found by *Rahimasoom Reza*[34], which exceeded 23 Å.

3.5 Spro molecular dynamic test

The RMSD values of protein backbones in the presence of both ligands reveal higher stability of PLpro in the presence of C02 relative to C01, while the RMSD values get nearly comparable as the system stabilizes after 50 ns of MD run (**Fig. 8 (a)**). **Fig. 8** depicts the calculated Rg values for (v) C01-Spro and (iv) C02-Spro along the simulated time scale (b). C01-Spro shows a steady Rg value of 18.3, while C02-Spro varies between 18.3 and 20. The Rg plot shows somewhat lower

values in the case of C02-Spro, indicating that the protein is stabilised in combination with C02. The RMSF of each backbone atom in the (v) C01-Spro and (iv) C02-Spro was computed to study the flexibility of the backbone structure in the presence of both ligands. In the presence of ligand C02, the RMSF of the protein backbone Spro is significantly greater than that generated by C01 with the Mpro (Figure 8(c, d)). The stability of the hydrogen bond arrangement created between (v) C01-Spro and (iv) C02-Spro throughout the simulation at 300 K for the ligated system was investigated, and the results are shown in Figure 8. (d). The number of hydrogen bonds in the C01-Spro and C02-Spro complexes ranges between 340 and 400 from the starting position to the end of the MD run; however, this amount is insufficient in comparison to the other complexes. The complexes created between the C01 and C02 and PLpro are relatively less stable than the complexes formed with the two targets.

4. Conclusion

Viral drug targets are more prone to alterations, which eventually triggered our interest in searching for compounds that bind SARS-CoV-2 to three different targets considering the sudden outbreak of the pandemic. Molecular docking was carried out for 190 chloroquine derivatives with the three protein targets of SARS-CoV-2 namely: 6LU7 (major protease), 6W41 (spike protein), and 6W9C (papain-like protease: PLpro). The studied compounds were evaluated for in silico molecular docking and the results indicated that the two compounds C01 and C02 were proved to be great importance in ligand-receptor binding and extremely effective in suppressing all three SARS-CoV-2 targets (Mpro, PLpro, and Spro) with significant binding affinities. The chemical with PubChem ID 456355 exhibits a high affinity for all of our targets, particularly the Main protease. The strong cell membrane penetrating ability of the identified compounds is evident from the calculated log P values between -2 and 5. The binding amino acids that bind to our molecules are hydrophobic or polar in nature. Two catalytic residues, HIS41 and CYS145, as well as other residues like GLY143, CYS145, HIS163, HIS164, GLU166, PRO168, and GLN189, are extremely intriguing for suppressing the Main protease. Furthermore, to enhance the docking study for the identified compounds C01 and C02 (top ranked), molecular dynamic (MDs) simulation was conducted for 50 ns and the results revealed that the two compounds C01 and C02 are particularly stable in complexing with the main protease of SARS-COV-2 and PLpro, whereas C02 is stable with the SARS-CoV-2 spike protein.

To conclude, these two compounds of chloroquine derivatives C01 and C02 stated in the present work could be a promising candidate for further drug discovery research against SARS-CoV-2 and assessed in vitro and in vivo studies to help accelerating research to halt the global spread of the Corona Virus and similar diseases.

Funding

The authors declare that no funds, grants, or other support were received during the preparation of this manuscript.

Competing Interests

The authors have no relevant financial or non-financial interests to disclose.

Conflicts of interest: The authors declare no conflict of interest.

Availability of data and material

All data generated or analyzed during this study are included in this published article.

Code availability

The calculations were performed using Schrodinger software [Canvas, Schrödinger, LLC, New York, NY, 2020]. Schrödinger Suite: LigPrep, version 2.5; Schrödinger, LLC: New York, 2012.

References

1. Achan, J., Talisuna, A. O., Erhart, A., Yeka, A., Tibenderana, J. K., Baliraine, F. N., et al. (**2011**) Quinine, an old anti-malarial drug in a modern world: role in the treatment of malaria. *Malar J. 10*, 144. DOI: 10.1186/1475-2875-10-144.
2. Magdalini A., Julija M., Enrico P., John H. (**2022**) The Coronavirus pandemic – 2022: Viruses, variants and vaccines. *Cytokine Growth Factor Rev., 36*, 1-9. DOI: 10.1016/j.cytogfr.2022.02.002.
3. Erikstrup, C., Hother, C. E., Pedersen, O. B. V., Mølbak, K., Skov, R. L., Holm, D. K., et al. (**2020**). Estimation of SARS-CoV-2 infection fatality rate by real-time antibody screening of blood donors. *Clin. Infect. Dis, 27*, 249-253. DOI: 10.1093/cid/ciaa849.
4. Chen, Y., Shen, T., Zhong, L., Liu, Z., Dong, X., Huang, T., ... & Xiao, H. (2020). Research progress of chloroquine and hydroxychloroquine on the COVID-19 and their potential risks in clinic use. *Front. Pharmacol*, *11*, 1167.
5. ul Qamar, M. T., Alqahtani, S. M., Alamri, M. A., & Chen, L. L. (**2020**). Structural basis of SARS-CoV-2 3CLpro and anti-COVID-19 drug discovery from medicinal plants. *J. Pharm. Anal.*, *10*(4), 313-319.

6. Anand K., Ziebuhr J., Wadhwani P., & Mesters JR. **(2014)** Coronavirus Main Proteinase (3CLpro) Structure: Basis for Design of Anti-SARS Drugs. Hilgenfeld. Science (New York, N.Y.), 300 (5626), 1763–1767. DOI: 10.1126/science.1085658.
7. Yang, H., Yang, M., Ding, Y., Liu, Y., Lou, Z., Zhou, Z., ... & Rao, Z. (**2003**) The crystal structures of severe acute respiratory syndrome virus main protease and its complex with an inhibitor. *Proceedings of the National Academy of Sciences*, *100*(23), 13190-13195.
8. Kim, S., Chen, J., Cheng, T., Gindulyte, A., He, J., He, S., ... & Bolton, E. E. (**2019**) PubChem 2019 update: improved access to chemical data. *Nucleic Acids Res.*, *47*(D1), D1102-D1109. DOI: 10.1093/nar/gky1033.
9. Duan, J., Dixon, S. L., Lowrie, J. F., & Sherman, W. (2010). Analysis and comparison of 2D fingerprints: insights into database screening performance using eight fingerprint methods. *J. Mol. Graph Model*, *29*(2), 157-170.
10. Jin, Z., Du, X., Xu, Y., Deng, Y., Liu, M., Zhao, Y., ... & Yang, H. (**2020**) Structure of Mpro from SARS-CoV-2 and discovery of its inhibitors. *Nature*, *582*(7811), 289-293.
11. DOI: 10.1038/s41586-020-2223-y.
12. Yuan M., Wu NC., Zhu X., et al., **(2020)** A highly conserved cryptic epitope in the receptor-binding domains of SARS-CoV-2 and SARS-CoV. *Science, 368*, 630–633. DOI: 10.1126/science.abb7269.
13. Osipiuk J., Jedrzejczak R., Tesar C., Endres M., Stols L., Babnigg G., Kim Y., Michalska K., Joachimiak A., **(2020)** The crystal structure of papain-like protease of SARS CoV-2. Worldwide PDB Protein Data Bank, 01, 1–14. DOI: 10.2210/pdb6w9c/pdb.
14. Burley SK., Berman HM., Christie C., Duarte JM., Feng Z., Westbrook J. (**2018**) RCSB Protein Data Bank: sustaining a living digital data resource that enables breakthroughs in scientific research and biomedical education. *Protein Sci, 27*(1), 316–330. DOI :10.1002/pro.3331
15. MJ. Vincent, E. Bergeron, S. Benjannet, et al., **(2005)** Chloroquine is a potent inhibitor of SARS coronavirus infection and spread.*Virol. J*, *2*, 69. DOI: 10.1186/1743-422X-2-69.
16. He, Z., Chen, L., You, J., Qin, L., & Chen, X. (**2009**). Antiretroviral protease inhibitors potentiate chloroquine antimalarial activity in malaria parasites by regulating intracellular glutathione metabolism. *Exp. Par.*, *123*(2), 122-127. DOI: 10.1016/j.exppara.2009.06.008.
17. Sastry GM., Adzhigirey M., Sherman W., (2013) Protein and ligand preparation: parameters, protocols, and influence on virtual screening enrichments. *Journal of computer-aidedmolecular design*, 27 (3), 221–234. DOI: 10.1007/s10822-013-9644-8.
18. Zhang L., Lin D., Sun X., et al. **(2020)** Crystal structure of SARS-CoV-2 main protease provides a basis for design of improved α-ketoamide inhibitors Science (New York, N.Y.) 368, 6489, 409–412. https://doi. org/10.1126/science.abb3405.
19. Arya R., Das A., Prashar V., Kumar M., **(2020)** Potential inhibitors against papain-like protease of novel coronavirus (SARS-CoV-2) from FDA approved drugs. *J. Biological and Medicinal Chemistry.* DOI: 10.26434/chemrxiv.11860011.v1.
20. Shang J., Ye G., Shi K., et al, **(2020)** Structural basis of receptor recognition by SARS-CoV-2. *Nature, 581*(7807), 221–224. DOI: 10.1038/s41586-020-2179-y.
21. Kim S., Thiessen PA., Bolton EE., et al, **(2016)** PubChem Substance and Compound databases *Nucleicacids research, 44*, D1202-13. DOI: 10.1093/nar/gkv951.
22. Genheden S., Ryde U., **(2015)** The MM/PBSA and MM/GBSA methods to estimate ligand-binding affinities. Expert Opinion on Drug Discovery 10(5), 449–461. DOI: 10.1517/17460441.2015.1032936.
23. Wang J., Morin P., Wang W., Kollman PA., **(2001)** Use of MM-PBSA in Reproducing the Binding Free Energies to HIV-1 RT of TIBO Derivatives and Predicting the Binding Mode to HIV-1 RT of Efavirenz by Docking and MM-PBSA. *J Am Chem Soc*, 123(22), 5221–5230. DOI: 10.1021/ja003834q.
24. Hou T., Wang J., Li Y., Wang W., **(2011)** Assessing the Performance of the MM/PBSA and MM/GBSA Methods. 1. The Accuracy of Binding Free Energy Calculations Based on Molecular Dynamics Simulations, J. Chem Inf Model, 51(1), 69–82. DOI: 10.1021/ci100275a.
25. Sitkoff D., Sharp KA., Honig B., **(1994)** Accurate Calculation of Hydration Free Energies Using Macroscopic Solvent Models. *J. Phys Chem*, 98(7), 1978–1988. DOI: 10.1021/j100058a043.
26. Wang J., Hou T., (2012) Develop and Test a Solvent Accessible Surface Area-Based Model in Conformational Entropy Calculations, J. Chem Inf Model, 52(5), 1199–1212 (2012). DOI: 10.1021/ci300064d.
27. Turner P. J. C. f. C., **(2005)** Land-Margin Research, and Technology, B., OR. XMGRACE, Version 5.1. 19.
28. Lipinski CA., Lombardo F., Dominy BW., Feeney PJ., **(1997)** Experimental and computational approaches to estimate solubility and permeability in drug discovery and development settings, *Advanced Drug Delivery Reviews*, 23, 3–25. DOI: 10.1016/S0169-409X(96)00423-1.
29. Ibrahim IM., Abdelmalek DH., Elshahat ME., Elfiky AA., **(2020)** COVID-19 spike-host cell receptor GRP78 binding site prediction, *Journal of infection,* 80(5),554–562. DOI: 10.1016/j.jinf.2020.02.026.
30. Mcclain CB., Vabret N., **(2020)** SARS-CoV-2: the many pros of targeting PLpro, *Signal Transduction and Targeted Therapy,* 5(1), 223. DOI: 10.1038/s41392-020-00335-z.
31. Rut W., Lv Z., Zmudzinski M., et al., **(2020)** Activity profiling and crystal structures of inhibitor-bound SARS-CoV-2 papain-like protease: A framework for anti–COVID-19 drug design, *Science Advances*, 6(42). DOI: 10.1126/sciadv.abd4596.

32. V. Gramany, FI. Khan, A. Govender, et al. **(2016)** Cloning, expression, and molecular dynamics simulations of a xylosidase obtained from Thermomyces lanuginosus, *J. Biomolecular Structure and Dynamic*s, *34*(8), 1681–1692. DOI: 10.1080/07391102.2015.1089186.
33. Beg A., Khan FI., Lobb KA. , et al., **(2019)** High throughput screening, docking, and molecular dynamics studies to identify potential inhibitors of human calcium/calmodulin-dependent protein kinase IV, *J. Biomolecular Structure and Dynamics*, 37(8), 2179–2192. DOI: 10.1080/07391102.2018.1479310.
34. Shubham S., Pakhuri M., Omprakash S., et al., **(2019)** Computationally guided identification of Akt-3, a serine/threonine kinase inhibitors: Insights from homology modelling, structure-based screening, molecular dynamics and quantum mechanical calculations, *J. biomolecular structure and dynamics, 38*(14), 4179–4188. DOI: 10.1080/07391102.2019.1675536.
35. Islam R., Parves R., Paul AS., et al., **(2020)** A molecular modeling approach to identify effective antiviral phytochemicals against the main protease of SARS-CoV-2, *J. biomolecular structure and dynamics, 39*(9), 3213–3224. DOI: 10.1080/07391102.2020.1761883.
36. Cruz Jorddy N., Costa F. S., José Khayat S., Kuca A., Barros A. L. , Carlos Neto A. M. J. C, **(2019)** Molecular dynamics simulation and binding free energy studies of novel leads belonging to the benzofuran class inhibitors of Mycobacterium tuberculosis Polyketide Synthase 13, *J. Biomol. Struct. Dyn.*, *37*(6), 1616–1627. DOI: 10.1080/07391102.2018.1462734.